Palaeontologia Electronica
palaeo-electronica.org

New look at *Concavicaris woodfordi* (Euarthropoda: Pancrustacea?) using micro-computed tomography

Thomas Laville, Thomas A. Hegna, Marie-Béatrice Forel, Simon Darroch, and Sylvain Charbonnier

ABSTRACT

Known from at least the Silurian to the Cretaceous, Thylacocephala is an enigmatic fossil euarthropod ingroup, often allied with Pancrustacea. Previous studies show that thylacocephalans are characterized by a folded protective shield, hypertrophied compound eyes, three pairs of raptorial appendages, a posterior trunk comprised of eight to 22 segments bearing appendages, and eight pairs of gills. Despite this knowledge of their anatomy, many questions remain, especially surrounding the anatomy of Paleozoic representatives.

The Upper Devonian Woodford Shale (upper Famennian, Oklahoma, USA) has yielded several fossil euarthropods, including two species of Thylacocephala: *Concavicaris elytroides* and *Concavicaris woodfordi.* Here, we use micro-computed X-ray tomography to re-explore the anatomy of the holotype of *C. woodfordi*, illustrating fine details of the shield structure, of the circulatory, digestive and reproductive systems, and of the appendages. A marginal fold of the shield as well as an inner layer are described for the first time in a thylacocephalan. *Concavicaris woodfordi* shares similarities with *Concavicaris submarinus*, another Famennian species, including the morphology of the shield and the internal anatomy. It also displays a similar organisation as Mesozoic taxa, such as *Dollocaris ingens*. All of this provides important information that will be crucial to reconstruct the evolution and the affinities of Thylacocephala.

Thomas Laville. Muséum national d'Histoire naturelle, Centre de Recherche en Paléontologie-Paris (UMR7207), MNHN-Sorbonne Université-CNRS, Paris, France and Biogéosciences, UMR 6282- CNRS, Université Bourgogne Franche-Comté, EPHE, Dijon, France. Corresponding author. thomas.laville@ecomail.fr
Thomas A. Hegna. Department of Geology and Environmental Science, State University of New York at Fredonia, New York, USA thomas.hegna@fredonia.edu
Marie-Béatrice Forel. Muséum national d'Histoire naturelle, Centre de Recherche en Paléontologie-Paris (UMR7207), MNHN-Sorbonne Université-CNRS, Paris, France. marie-beatrice.forel@mnhn.fr
Simon Darroch. Department of Earth and Environmental Sciences, Vanderbilt University, Nashville,

Final citation: Laville, Thomas, Hegna, Thomas A., Forel, Marie-Béatrice, Darroch, Simon, and Charbonnier, Sylvain. 2023. New look at *Concavicaris woodfordi* (Euarthropoda: Pancrustacea?) using micro-computed tomography. Palaeontologia Electronica, 26(1):a1. https://doi.org/10.26879/1218
palaeo-electronica.org/content/2023/3735-new-look-at-concavicaris-woodfordi

Tennessee, USA. simon.a.darroch@vanderbilt.edu
Sylvain Charbonnier. Muséum national d'Histoire naturelle, Centre de Recherche en Paléontologie-Paris (UMR7207), MNHN-Sorbonne Université-CNRS, Paris, France. sylvain.charbonnier@mnhn.fr

Keywords: Thylacocephala; Late Devonian; virtual Paleontology; internal anatomy; soft-parts preservation; shield structures

Submission: 15 February 2022. Acceptance: 2 December 2022.

INTRODUCTION

Thylacocephalans are enigmatic euarthropods, often regarded as an ingroup of Pancrustacea Zrzavý and Štys, 1997 (see Haug et al., 2014; Vannier et al., 2016; Broda and Zatoń, 2017). They are characterized by distinct anatomical features: a folded shield enveloping most of the body, hypertrophied compound eyes, three pairs of raptorial appendages, a trunk made of eight up to 22 segments bearing appendages, and eight pairs of gills (Schram, 2014). Despite recent work providing important information on their anatomy and tagmosis (Haug et al., 2014; Vannier et al., 2016; Broda and Zatoń, 2017; Jobbins et al., 2020), the phylogenetic affinities of Thylacocephala Pinna, Arduini, Pesarini and Teruzzi, 1982 are still unclear. They have been proposed to be related to phyllocarids (e.g., Cooper, 1932; Chlupáč, 1963), stomatopods (as larval forms; e.g., Hilgendorf, 1885), thecostracans (Pinna et al., 1985), and more recently to malacostracans (Secrétan, 1985; Vannier et al., 2016) and remipedes (Haug et al., 2014).

Known from at least the Silurian (Haug et al., 2014) up to the Late Cretaceous (e.g., Schram et al., 1999; Lange et al., 2001; Charbonnier et al., 2017), thylacocephalans were relatively diverse in the Devonian (Table 1). Fourteen species have been formally described from 10 different localities corresponding to a wide variety of depositional environments, from tidal channels to offshore environments. Devonian representatives have provided important insight into the morphology of thylacocephalans, especially into their segmentation (Briggs and Rolfe, 1983; Stigall and Hendricks, 2007), their internal anatomy (Jobbins et al., 2020), and their ornamentation (Broda and Zatoń, 2017; Broda et al., 2020). Recent knowledge on the internal anatomy of Devonian thylacocephalans has been acquired thanks to the use of micro-computed X-ray tomography (µCT): 3D rendering of *Concavicaris submarinus* Jobbins et al., 2020 from the middle Famennian of Morocco revealed unknown structures such as putative reproductive organs. It was only the second thylacocephalan species studied using µCT imagery, after *Dollocaris ingens* Van Straelen, 1923, from the Callovian La Voulte-sur-Rhône Lagerstätte (Vannier et al., 2016).

In order to expand our knowledge on the anatomy of Thylacocephala, it is necessary to apply such approaches more commonly to thylacocephalans. In this study, we re-examine the holotype of *Concavicaris woodfordi* (Cooper, 1932) using µCT in order to explore its internal and external anatomy. This species is one of the rare thylacocephalan with specimens preserved in 3D, which makes it a good candidate for a µCT study. The detailed 3D rendering obtained via µCT offers new insights into the anatomy of thylacocephalans.

GEOLOGICAL SETTING

The Upper Devonian Woodford Shale crops out in the Arbuckle Mountains, southern Oklahoma, USA (Figure 1A, B). Based upon conodont biostratigraphy, the unit ranges from the Late Devonian (Frasnian) to the Early Carboniferous (Mississippian; Over, 1992). During the Devonian, the Arbuckle Mountains were part of a broad marine shelf. During the Early Devonian, sedimentation was mainly dominated by carbonates. In the Frasnian (Late Devonian), the character of sedimentation changed with fine-grained siliciclastics dominant until the Early Carboniferous. This led to the formation of the Woodford Shale.

The Woodford Shale is a fine-grained siliciclastic unit that ranges in thickness from 30 m to >60 m. It consists of alternating brown, black, and grey mudstones and shale beds with interbedded phosphatic layers and phosphatic concretions in the upper part (Figure 1C; Kirkland et al., 1992; Over, 1992; Roberts et al., 1992). The Woodford Shale was deposited in an offshore basin characterized by stagnant water masses and relatively high salinity (Over, 1992; Romero and Philp, 2012).

Macrofossils are preserved in lenticular phosphatic concretions (Figure 1C; Over, 1992). In addition to conodonts, radiolarians,

TABLE 1. Diversity and depositional settings of Devonian thylacocephalans.

Series	Age	Occurrence	Species	Environment	Lithology	References
Early Devonian	Late Emsian	Várův mill and Pekárkův mlýn, Czech Republic	*Concavicaris desiderata* (Barrande 1872)	subtidal quiet environment	calcareous intercalation in black shales	Barrande, 1872; Chlupáč, 1963
Middle/Late Devonian	Na	Route 30, Grand Gorge, New York, USA	*Concavicaris*? sp. indet.	tidal channels, brackish floodplain	micaceous siltstone	Stigall and Hendricks, 2007
Late Devonian	Early Frasnian	Gogo station, Fitzroy basin, Australia	*Concavicaris campi* Briggs and Rolfe, 1983	inter-reef basin, marginal slope	calcareous concretions in black shales	Briggs and Rolfe, 1983; Broda et al., 2020
			Concavicaris glenisteri Briggs and Rolfe, 1983	inter-reef basin, marginal slope	calcareous concretions in black shales	Briggs and Rolfe, 1983; Broda et al., 2020
			Concavicaris milesi Briggs and Rolfe, 1983	inter-reef basin, marginal slope	calcareous concretions in black shales	Briggs and Rolfe, 1983; Broda et al., 2020
			Concavicaris playfordi Briggs and Rolfe, 1983	inter-reef basin, marginal slope	calcareous concretions in black shales	Briggs and Rolfe, 1983; Broda et al., 2020
			Harrycaris whittingtoni Briggs and Rolfe, 1983	inter-reef basin, marginal slope	calcareous concretions in black shales	Briggs and Rolfe, 1983; Broda et al., 2020
			"Ainiktozoon" sp.	Lagoonal environment	thin-bedded, dark limestones	Heidtke and Krätschmer, 2001
	Fammenian	Hády quarry, Brno, Czech Republic	*Concavicaris incola* Chlupáč, 1963	hemipelagic slope	black, calcareous shales	Chlupáč, 1963; Broda et al., 2020
	Early Fammenian	Hády quarry, Brno, Czech Republic	*Concavicaris martinae* Broda et al., 2020	low-energy slope, well below storm-wave base	black shales	Broda et al., 2020
		Holy Cross Mountains, Poland	*Concavicaris pikae* Broda et al., 2020	deep shelf, under the storm wave-base level	thin-bedded, laminated, dark, carbona-ceous shales	Zatoń et al., 2014; Broda and Zatoń, 2017; Broda et al., 2020
		Woodruff Creek, Nevada, USA	*Concavicaris woodruffensis* Broda et al., 2020	shallow marine shelf	dark grey mudstones	Briggs and Rolfe, 1983; Broda et al., 2020
	Middle Fammenian	Madène El Mrakib, Anti-Atlas, Morocco	*Concavicaris submarinus* Jobbins et al., 2020	epicontinental basin	haematite-rich concretions in claystones	Jobbins et al., 2020
		Kattensiepen quarry, Rhenish massif, Germany	*Suttropcaris bottkei* Koch et al., 2003	Na	bituminous calcareous nodules in black shales	Koch et al., 2003; Rolfe and Dzik, 2006
	Late Fammenian	Cleveland shale, Ohio, USA.	*Concavicaris* aff. *bradleyi*	epicontinental foreland basin, below storm-wave base	black shales	Briggs and Rolfe, 1983
		Arbuckle mountain, Oklahoma, USA	*Concavicaris elytroides* (Meek, 1872)	offshore, deep, quiet-water settings basin	phosphatic concretions in black shales	Cooper, 1932
			Concavicaris woodfordi (Cooper, 1932)	offshore, deep, quiet-water settings basin	phosphatic concretions in black shales	Cooper, 1932; this paper

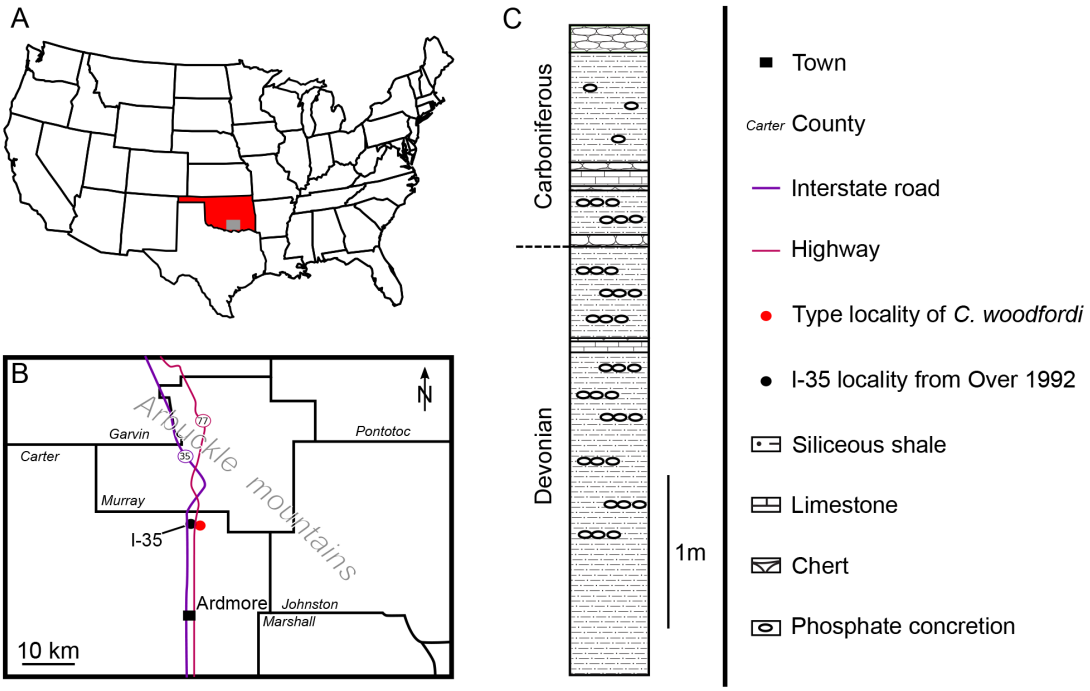

FIGURE 1. Position and geology of the fossil locality. **A,** Map of USA with the position of Oklahoma (red area) and of Arbuckle Mountains (grey area). **B,** Map of Arbuckle mountains with the position of the type locality of *Concavicaris woodfordi* (Cooper, 1932). **C,** Section of the upper Woodford Shale at Interstate 35 road-cut section (I-35) (sec. 25, T2S, R2E, Arbuckle Mountains, Oklahoma, USA; redrawn after Over [1992]).

sponge spicules, ammonoid and nautiloid cephalopods as well as inarticulate brachiopods have been reported (Over, 1992). The Woodford Shale has also yielded some fossil euarthropods, including *Aciculopoda mapesi* Feldmann and Schweitzer, 2010, which is possibly the oldest dendrobranchiate shrimp, and two species of Thylacocephala: *Concavicaris elytroides* (Meek, 1872) and *Concavicaris woodfordi* (Cooper, 1932).

MATERIAL AND METHODS

Specimen

For the purpose of this study, we re-examined the holotype of *Concavicaris woodfordi*, which is stored in the paleontological collections of the National Museum of Natural History, Smithsonian Institution, Washington, DC (USNM PAL 112025). This specimen was collected along the east side of U.S. Highway 77, Arbuckle Mountains, Oklahoma, USA (sec.30, T2S, R2E; Cooper 1932; Figure 1C), and is the only known specimen.

Taphonomy. The specimen is preserved in 3 dimensions in a phosphatic concretion. Neither the anterior nor the posterior parts of the shield are preserved. Some soft-parts, including eyes, cephalic appendages, and part of the posterior trunk appendages are also not preserved. The tomographic data emphasize the differential preservation of the anatomical structures. Organs (circulatory and digestive systems) and appendages appear less dense in the tomograms, indicating a preservation in a low-density material or as empty mold. In contrast, the shield is preserved in a dense material, appearing black in the tomograms. An elongate veil-like structure, which is partly connected to the shield, appears formed of two dense layers separated by sediments. In its posterior part, it is only formed of dense material. The veil-like structure is slightly folded in its anterior part, appearing collapsed. It seems to have undergone a small clockwise rotation in its posterior part.

The whole specimen is filled with sediments of medium density (grey in the tomograms). At the back of the specimen, a particular infill seems to have occurred based on a denser material than the rest of the specimen. This particular infill is formed of rounded holes. The broken shield, the filling of the shield, the deformation of some structures and the loss of soft-parts indicate that the carcass was

probably affected by decay when lying on the seafloor, prior to the entombment in the phosphatic nodule.

Anatomical abbreviations. am, adductor muscles; cs, cylindrical structure; g, gills; gm, gastric muscles; hp, hepatopancreas; il, inner layer; lvp, latero-ventral pouch; mf, marginal fold; pl, pleural part; pt, posterior trunk; pta, posterior trunk appendages; r, rostrum; raptorial appendages; s, shield; so, shield outline; st, sternal part; sto, stomach; te, tergal part.

Measurements. We followed the scheme of measurements from Laville et al. (2021a). Measurements were done on the macro-photographs of the specimen using ImageJ2 (Schneider et al., 2012).

Measurements abbreviations. A_{ad}, antero-dorsal angle; A_{av}, antero-ventral angle; A_{pd}, postero-dorsal angle; A_{pv}, postero-ventral angle; l, length; l_r, length of rostrum; l_s, length of shield; l_w, length of shield without rostrum; h, height; h_a, anterior height; h_{max}, maximal height of shield; h_p, posterior height; w, width.

X-ray Microtomography

The specimen was micro-CT scanned using the North Star Imaging µCT scanner housed at Vanderbilt University (Tennessee, USA), and 1377 two-dimensional images were obtained with a voxel size of 46 µm at a voltage of 115 kV and current of 10 µA (Appendix 1); the volume was reconstructed using EFX-CT (North Star Imaging, Minnesota, USA). Rotation (178°), cropping and, conversion to 8-bit were applied to every slice prior to segmentation. Manual and semi-automatic segmentation were done using Mimics 24.0 Research Edition (Materialise; Appendix 1). Three-dimensional rendering and processing was done using Meshlab 2021.05 (GNU GPL 3.0; Cignoni et al., 2008). Video of the 3D rendering (Appendix 2) was constructed using Blender 2.93.1 (GNU GPL 3.0).

ANATOMY

Shield Morphology

The shield (s) appears to have a cylindrical shape (Figure 2) with a roughly oval-shaped cross-section (Figure 3). It is at least two times longer than high (Table 2). Both sides of the shield are convex (Figure 3). Rostrum and posterior margin are broken as is the dorsal part of the shield. Anterior margin is slightly slopping ventrally. Dorsal midline and ventral margin appear convex. Antero-ventral corner is rounded.

The ventral area of the shield is marked by a depression (Figures 2C, 3D–F). In transverse view, the ventral part of the shield is folded up on itself, forming a marginal fold, which appears well-mineralized. This latter is delimiting a cavity, which has a lunate outline in the anterior part of the shield (Figure 3A–C). This hollow becomes smaller and triangular posteriorly (Figure 3D–F).

Organs and Internal Structures

Inner layer. An elongated and widespread inner layer is located dorsally below the shield (il; Figures 3-5). It appears divided into two parts. The anterior one, which is attached to the marginal fold, has a shape similar to the shield (Figure 4A –C). This anterior part both dorsally and laterally envelops the soft-parts, but is open ventrally (Figure 6B, D).

The posterior part has a very different morphology: it is less wide and high than the anterior portion and unlike the anterior portion, it appears to be a closed structure (Figure 4D–F). It seems to have undergone a slight clockwise rotation, probably linked to the decay and settling of the organism. This posterior part has an almost square shape in cross-section. Its tergal part (te) has a large ridge centrally. This ridge is surrounded on each side by a fold, defining a narrow ridge (Figures 3C, D, 4D, E). The pleural parts (pl) are ventro-laterally oriented in their upper third. They became vertical in the middle and lower thirds. Finally, the sternal (st) area appears slightly concave. The posterior trunk appendages (see below) are connected to this ventral area (Figure 5F).

Digestive system. A large, semi-circular structure, oriented transversely to the body axis, is located in the anterior part of the shield (interpreted as stomach; sto; Figures 6, 7A–D). This structure is attached on its ventral ends to two rounded structures (interpreted as latero-ventral pouch; lvp). It appears wider near the putative gonads.

Gonads. Two, long plate-like structures (interpreted as gonads; go) are located below the dorsal area of the anterior part of the inner layer (Figures 6, 7A–D). They are 2.65 times longer than wide. They are laterally tilted, mirroring one another.

Gills. Eight pairs of lamellar structures are preserved (interpreted as gills; g; Figures 6, 7E–G). They are attached to the ventral side of the anterior part of the inner layer. They appear to form a fan, following the shape of the shield. The anterior structures are vertical while the posterior ones are almost horizontal.

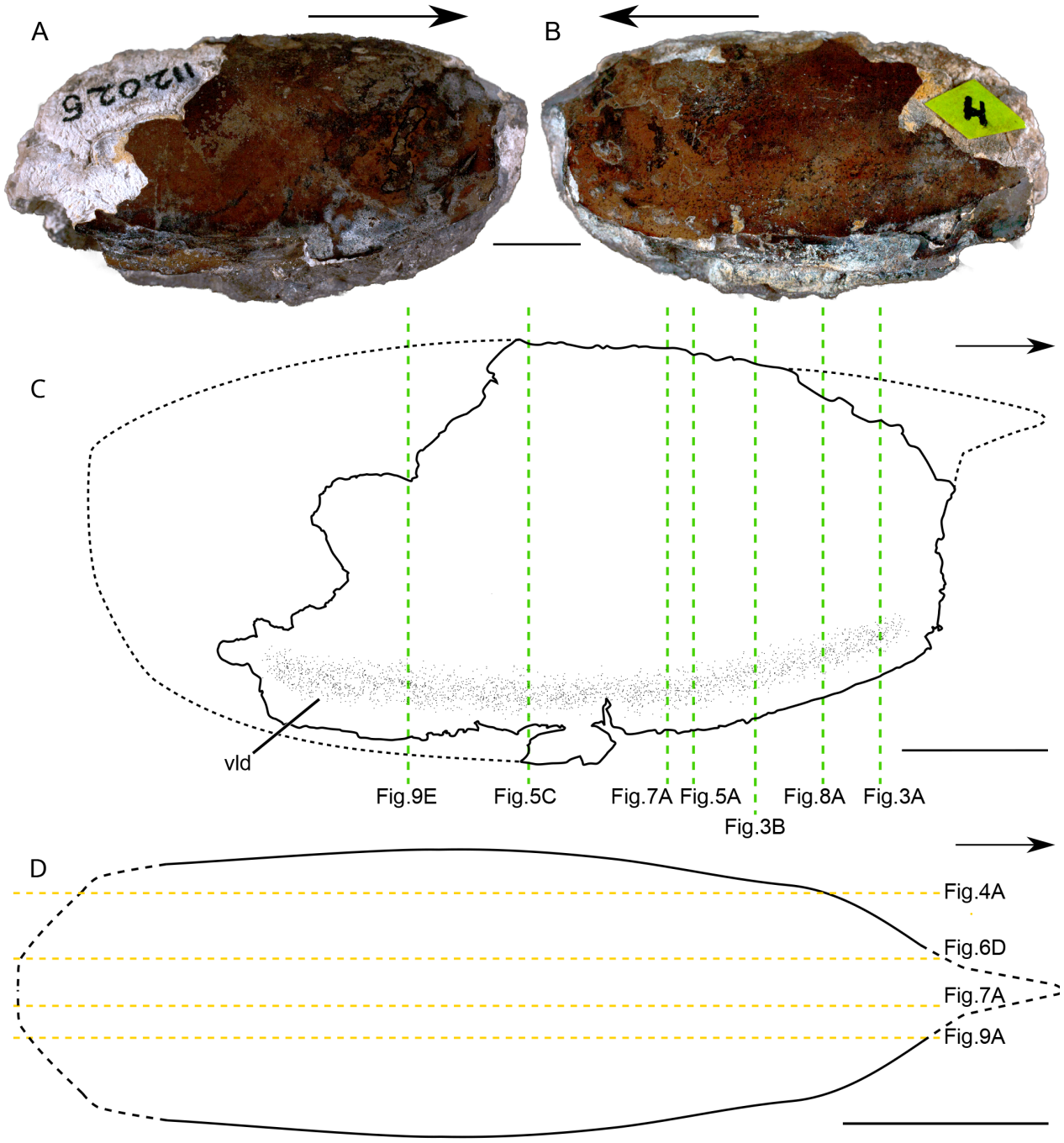

FIGURE 2. General view of *Concavicaris woodfordi* (Cooper, 1932). **A, B,** Right and left lateral views. **C,** line drawing (lateral view). **D,** location of virtual slices presented in the figures (dorsal view). Abbreviations: vld, ventro-lateral depression. Arrows indicate the anterior side of the specimen. Yellow doted lines indicate longitudinal sections. Green dotted lines indicate transversal sections. Scales: 10 mm. Photos: T. A. Hegna.

Longitudinal cylindrical structure. On the left of the shield, a longitudinal cylindrical structure is closely associated with the lamellar structure (cs; Figures 6, 7E–G). In its anterior part, the structure becomes medio-ventrally oriented.

Anterior fibrous structures. A mass of fibrous structures is located below the semi-circular structure (interpreted as gastric muscle; gm; Figure 8A–C). Their orientation and structure are not clear due to their poor preservation.

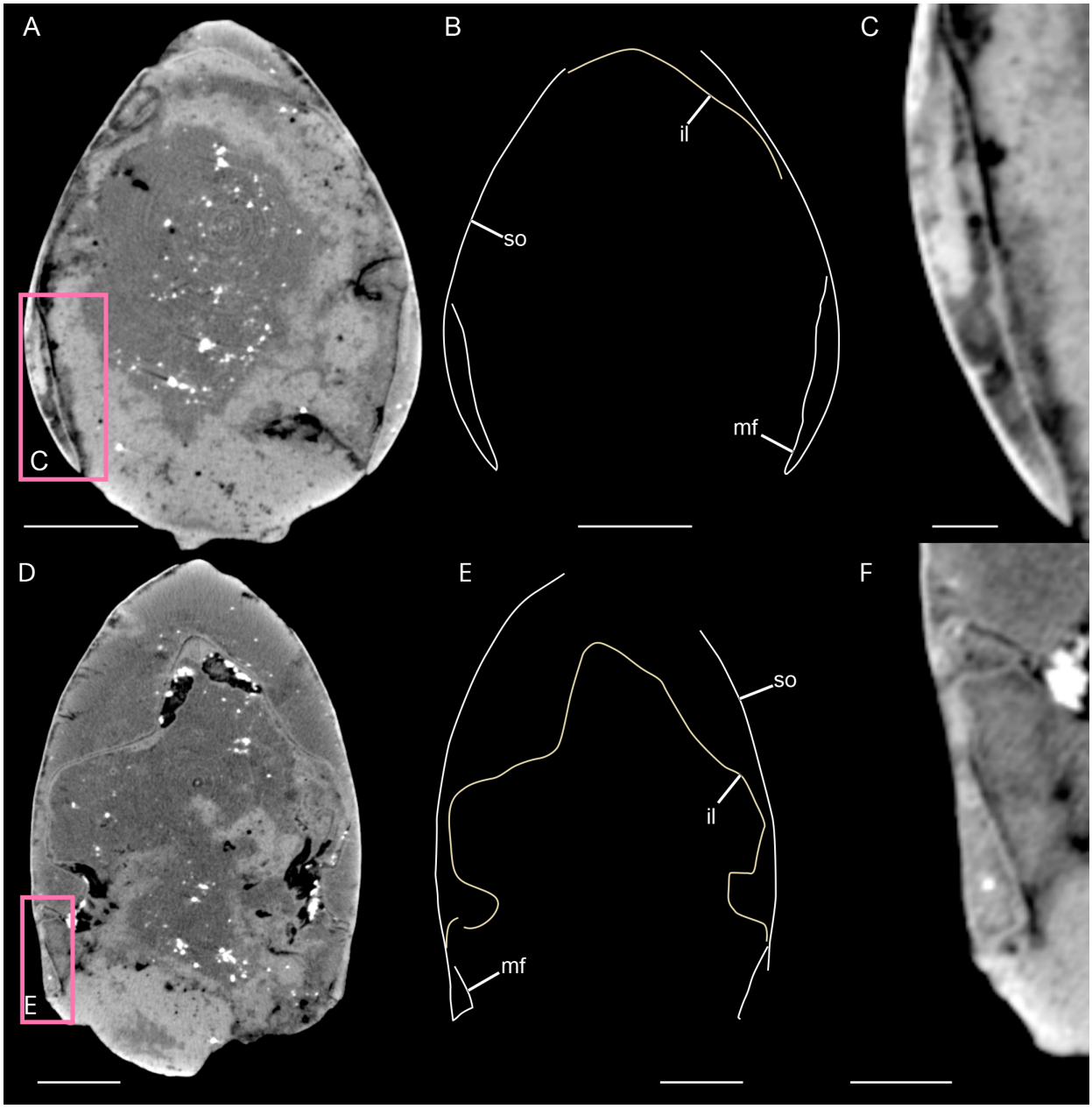

FIGURE 3. Marginal fold of *Concavicaris woodfordi* (Cooper, 1932). **A, B,** anterior part of the shield (tomogram and drawing). **C,** close-up of marginal fold in the anterior part of the shield (tomogram). **D, E,** middle part of the shield (tomogram and drawing). **F,** close-up of marginal fold in the middle part of the shield (tomogram). Abbreviations: il, inner layer; mf; marginal fold; so, shield outline. Scales: A, B, D, E, 5 mm; C, F, 1 mm.

TABLE 2. Measurements on the shield of *Concavicaris woodfordi* (Cooper, 1932). Abbreviations: l_r, length of the rostrum; l_s, length of the shield; l_w, length of the shield without the rostrum; h_a, anterior height; h_{max}, maximal height of the shield; h_p, posterior height; w, width.

l_s	l_w	l_r	h_a	h_{max}	h_p	w
>54.2 mm	Na	Na	~11.3 mm	~25.3	>7.7 mm	~15.6 mm

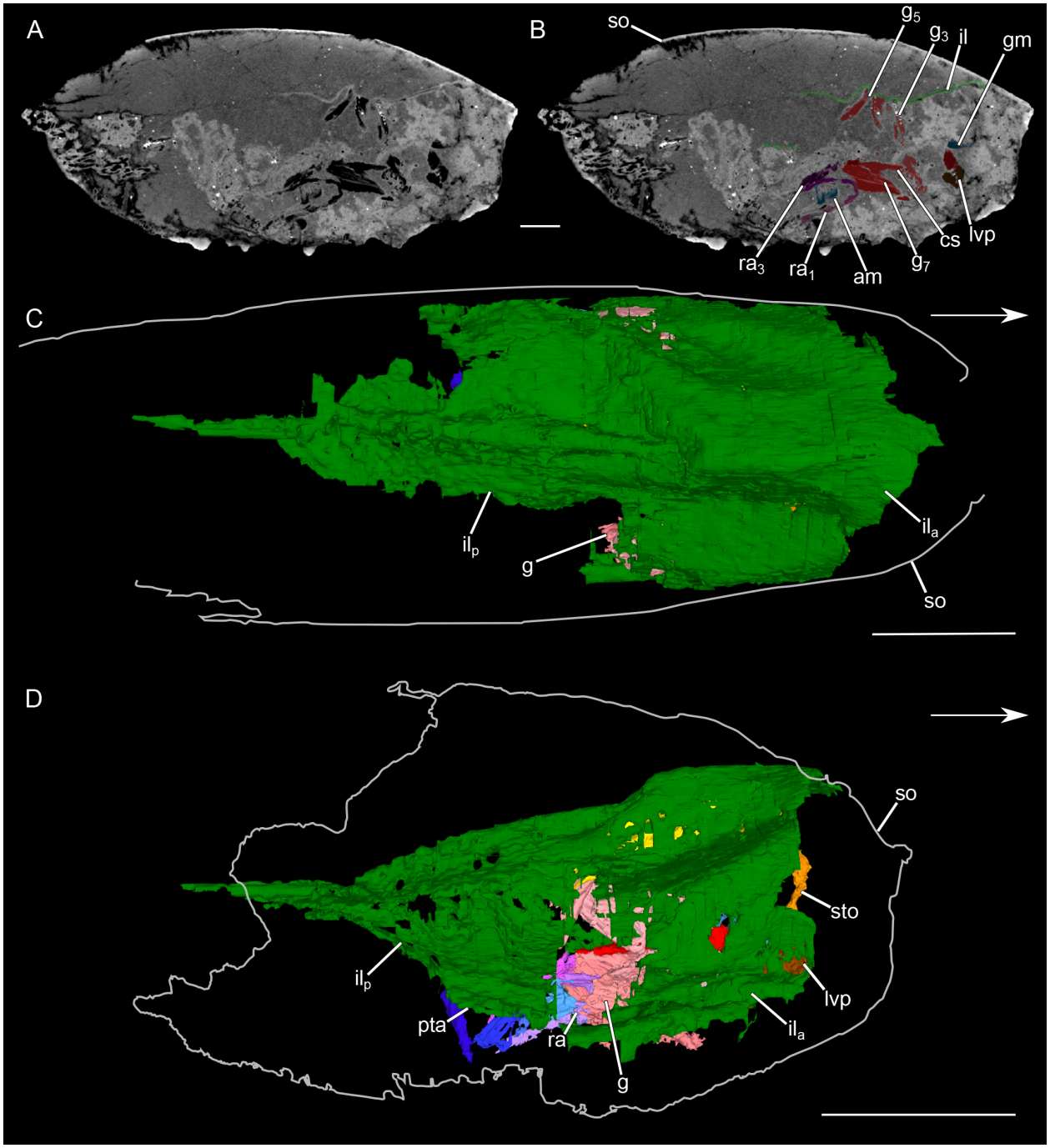

FIGURE 4. Anatomy of *Concavicaris woodfordi* (Cooper, 1932). **A,** longitudinal virtual section. **B,** longitudinal virtual section (colour-marked). **C,** dorsal view (3D rendering). **D,** lateral view (3D rendering). Abbreviations: am, adductor muscles; cs, cylindrical structure; $g_{2–7}$, gills; gm, gastric muscles;il_a, anterior part of the inner layer; il_p, posterior part of the inner layer; lvp, latero-ventral pouch; pta, posterior trunk appendages; $ra_{1–3}$, raptorial appendages; so, shield outline; sto, stomach. Arrows indicate the anterior side of the specimen. Scales: 10 mm.

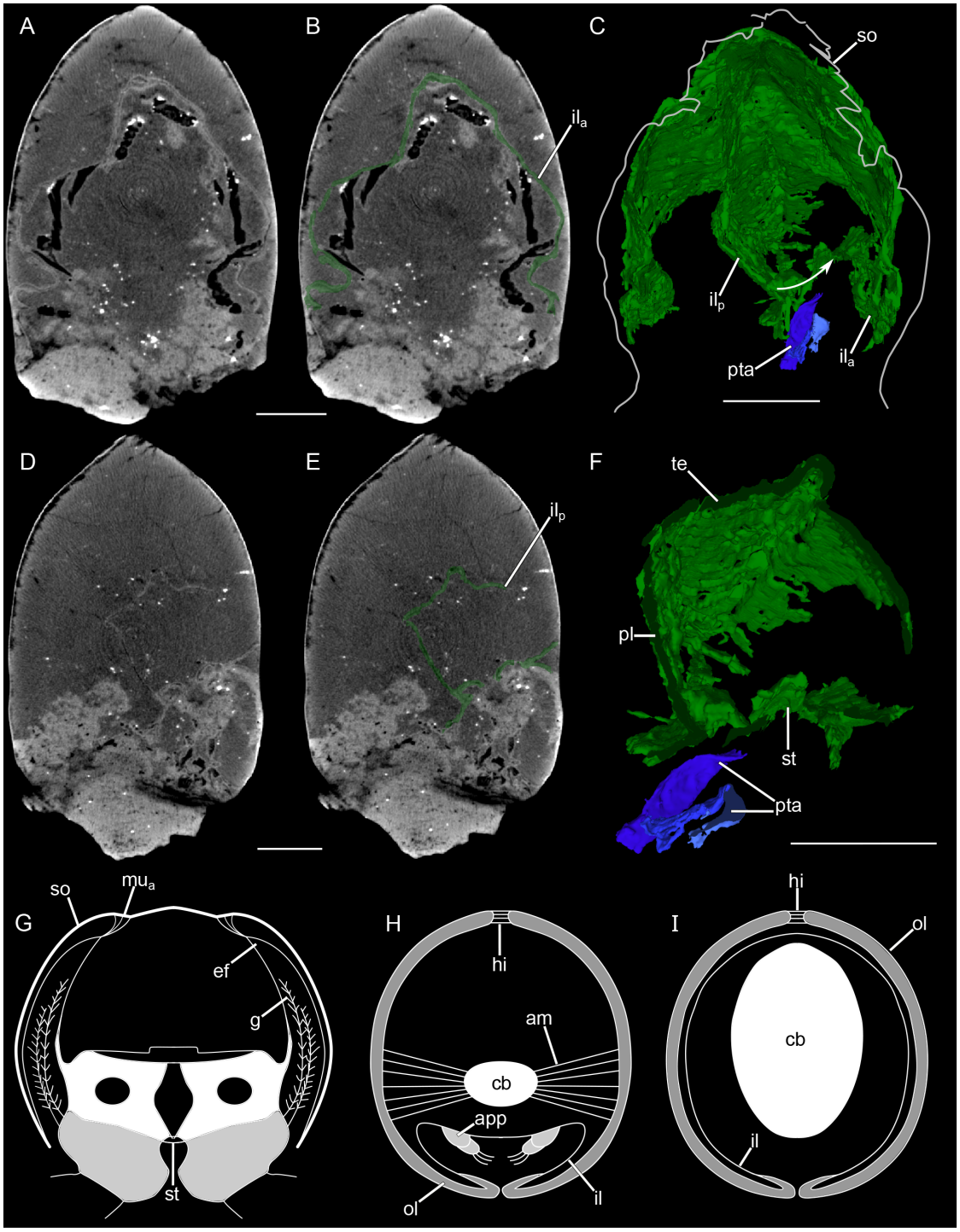

FIGURE 5. Inner layer of *Concavicaris woodfordi* (Cooper, 1932). **A–C,** anterior part of the specimen. **A,** tomogram (transversal slice). **B,** tomogram (transversal slice; colour-marked). **C,** anterior view (3D rendering). **D–F,** posterior part of the specimen. **D,** tomogram (transversal slice). **E,** tomogram (transversal slice; colour-marked). **F,** cross-section (3D rendering). **G,** cross-section of cephalothorax of a reptantian decapod (after Glaessner, 1969). **H, I,** cross-section of the carapace structure of a myodocopan (*Euphilomedes japonica* (Müller, 1890); after Yamada, 2019). **H,** attached region. **I,** duplicated region. Arrow indicates the rotation of the posterior part of the inner layer. Abbreviations: am, adductor muscles; app, appendage; cb, chitinous body; ef, epimeral fold; g, gills; hi, hinge; il, inner layer of the shield; il_a, anterior part of the inner layer; il_p, posterior part of the inner layer; mu_a, attractor muscles; ol, outer layer of the shield; pl, pleural part; pta, posterior trunk appendages; so, shield outline; st, sternal part; te, tergal part. Scales: 5 mm.

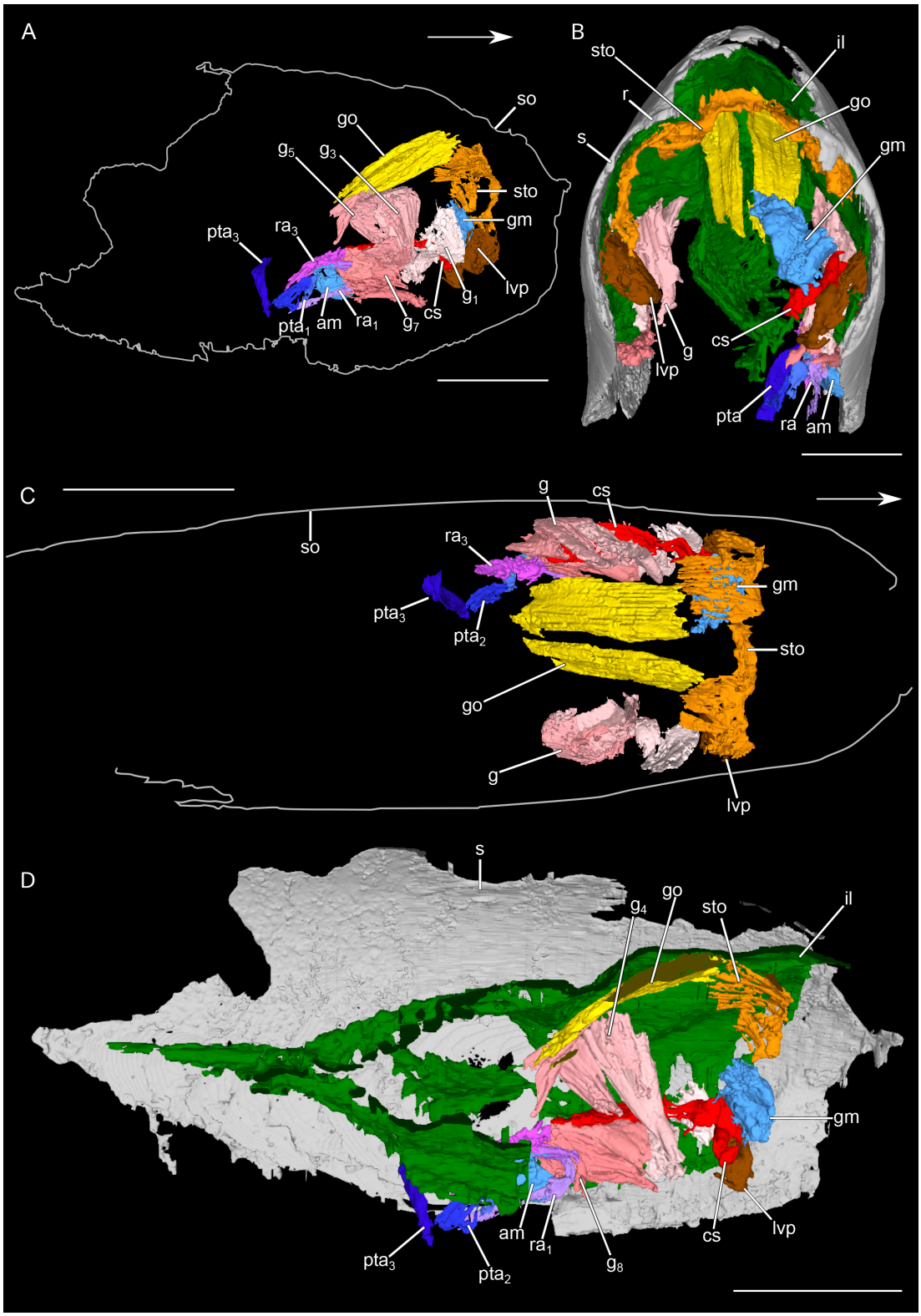

FIGURE 6. Internal anatomy of *Concavicaris woodfordi* (Cooper, 1932). **A,** right lateral view (3D rendering). **B,** anterior view (3D rendering). **C,** dorsal view (3D rendering). **D,** longitudinal section (3D rendering). Abbreviations: am, adductor muscles; cs, cylindrical structure; $g_{1–8}$, gills; gm, gastric muscles; go, gonads; lvp, latero-ventral pouch; $pta_{1–3}$, posterior trunk appendages; r, rostrum; $ra_{1, 3}$, raptorial appendages; s, shield; so, shield outline; sto, stomach. Arrows indicate the anterior side of the specimen. Scales: A, C, D, 10 mm; B, 5 mm.

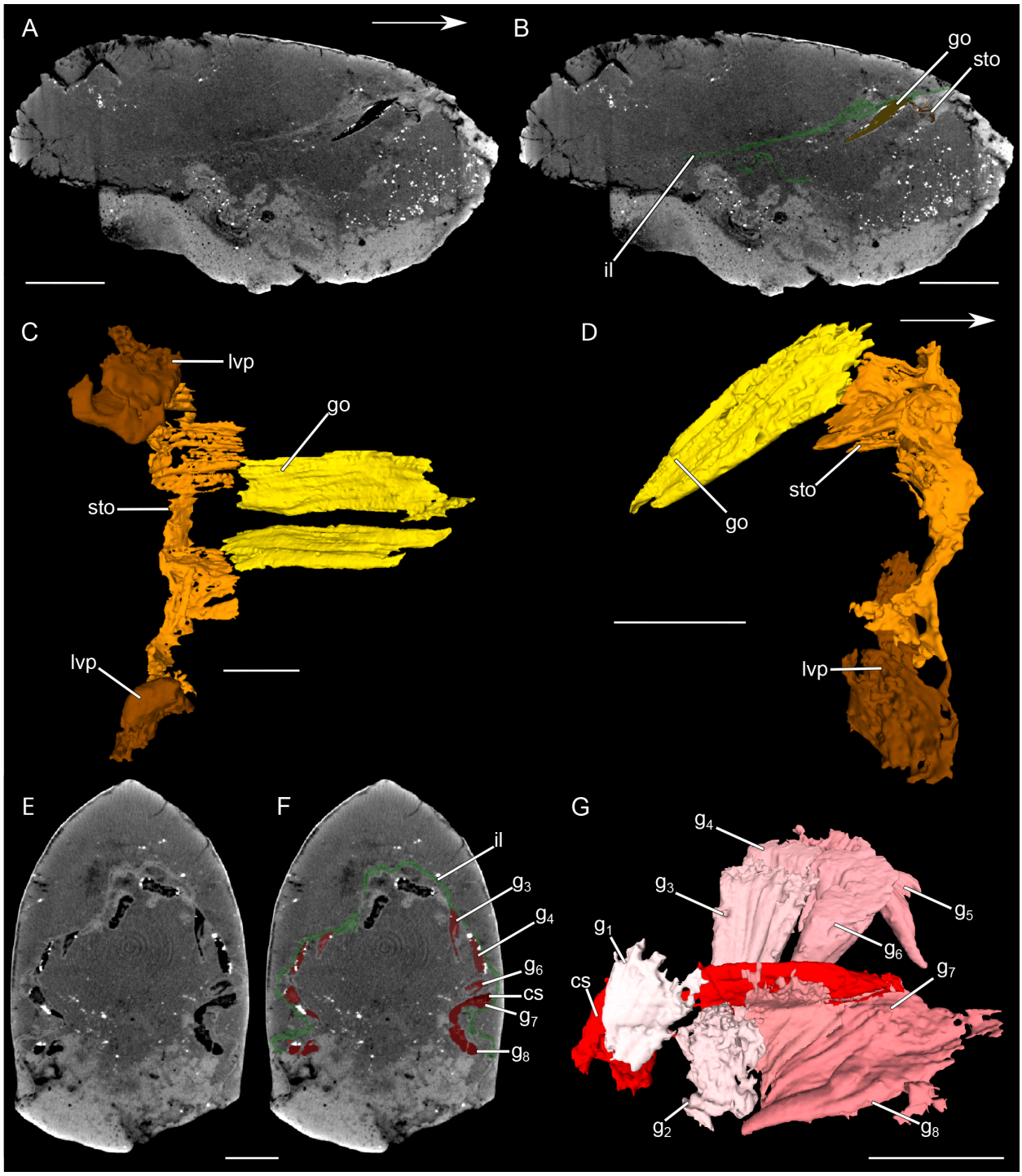

FIGURE 7. Digestive, reproductive, and circulatory systems of *Concavicaris woodfordi* (Cooper, 1932). **A,** longitudinal virtual section. **B,** longitudinal virtual section (colour-marked). **C, D,** digestive and reproductive systems (3D rendering). **C,** anterior view. **D,** right lateral view. **E, F, G,** circulatory system. **E,** tomogram. **F,** tomogram (colour-marked). **G,** 3D rendering of the left part. Abbreviations: cs, cylindrical structure; $g_{1–8}$, gills; go, gonads; il, inner layer; lvp, latero-ventral pouch; sto, stomach. Arrows indicate the anterior side of the specimen. Scales: A, B, 10 mm; C–G, 5 mm.

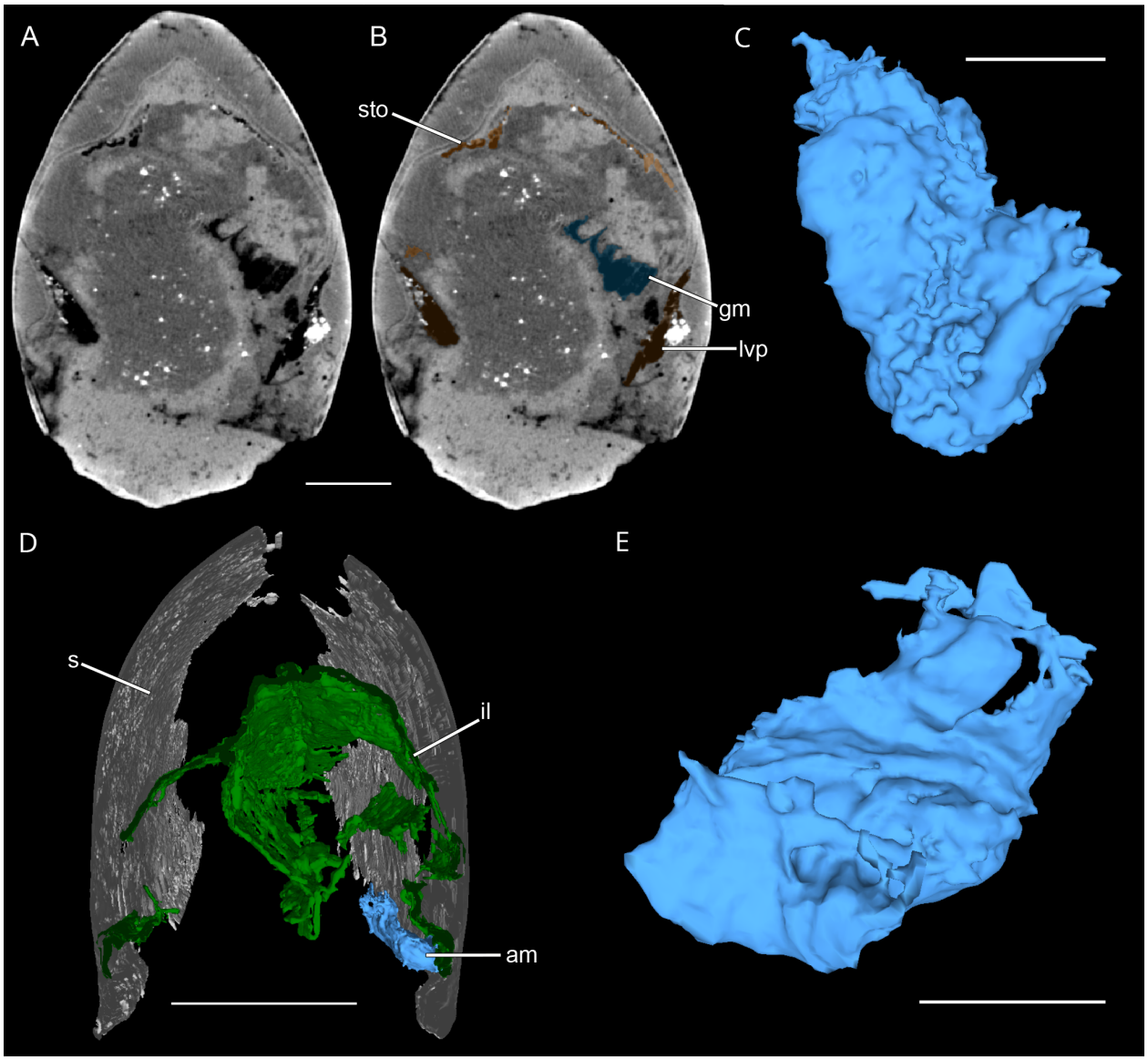

FIGURE 8. Muscular structures of *Concavicaris woodfordi* (Cooper, 1932). **A**, tomogram. **B,** tomogram (colour-marked). **C,** gastric muscles (3D rendering). **D,** cross-section (3D rendering). **E,** adductor muscles (3D rendering). Abbreviations: am, adductor muscle; gm, gastric muscles; il, inner layer; lvp, latero-ventral pouch; s, shield; sto, stomach. Scales: A, B, D, 5 mm; C, E, 2 mm.

Central fibrous structures. A mass of fibrous structures is lying posterior to the left lamellar structures (interpreted as adductor muscle; am; Figures 4A, B, 8D, E). These fibrous structures are connected to the shield (Figure 8D), where it appears divided into two parts.

Raptorial appendages. Posterior to the lamellar structures, three poorly preserved rectangular structures are oriented postero-dorsally (interpreted as raptorial appendages; ra; Figure 4A, B, 9A, B). They are associated with the anterior part of the inner layer. The first of these structures (ra_1) appears divided into at least two podomeres.

Posterior appendages. Close to the ventral area of the posterior area of the inner layer, three paddle-like structures (interpreted as posterior trunk appendages; pta) can be distinguished (Figure 9C–E). They are poorly preserved. They are antero-posteriorly flattened, and their lateral and medial sides form a carina. The proximal part of the appendages is anteriorly oriented while the distal one is laterally oriented.

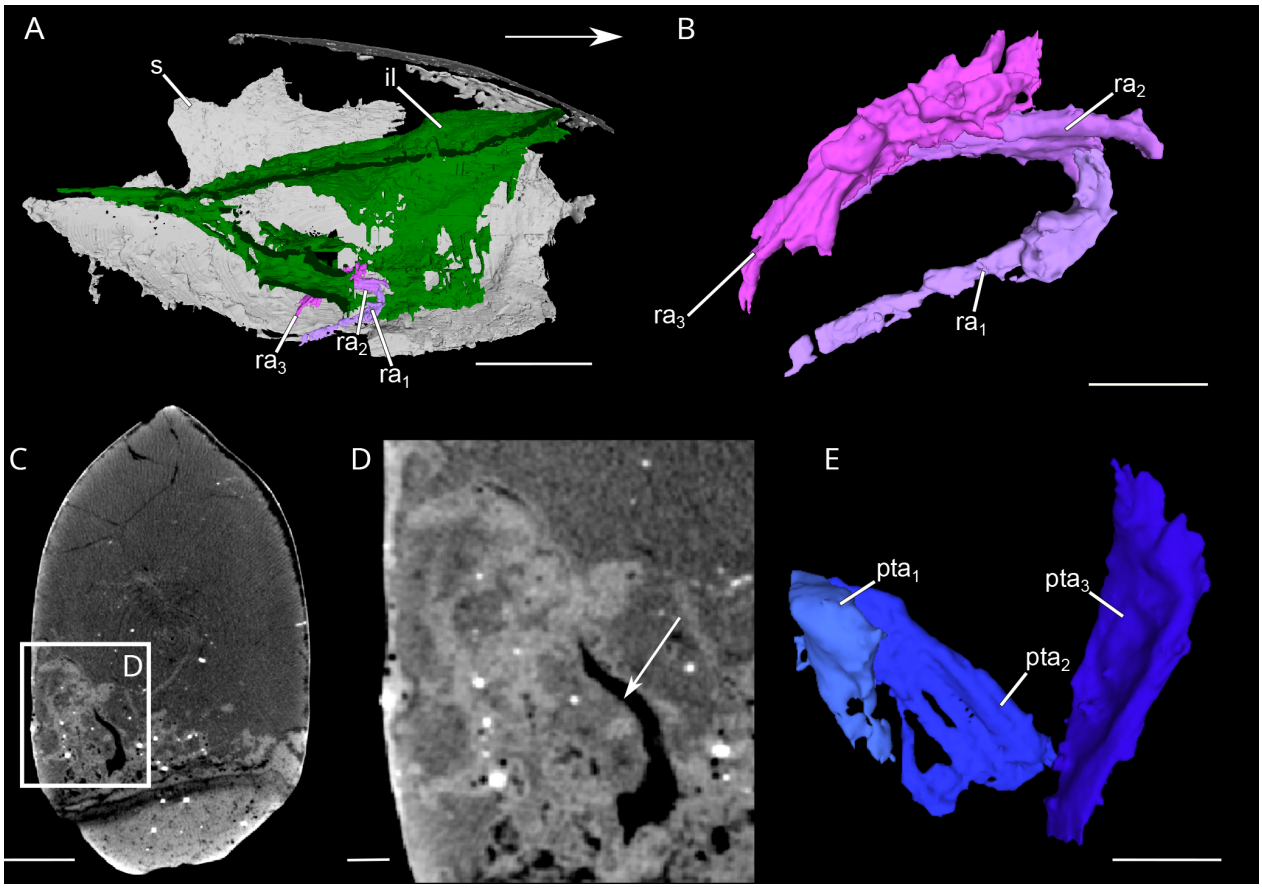

FIGURE 9. Appendages of *Concavicaris woodfordi* (Cooper, 1932). **A,** longitudinal section (3D rendering). **B,** raptorial appendages (3D rendering). **C,** tomogram. **D,** close-up of third posterior trunk appendage. **E,** posterior trunk appendages (3D rendering). Arrow indicates the third posterior trunk appendage. Abbreviations: il, inner layer; $pta_{1–3}$, posterior trunk appendages; $ra_{1–3}$, raptorial appendages; s, shield. Arrow indicates the anterior side of the specimen. Scales: A–C, 10 mm; D, G, 2 mm; E, 5 mm; F, 1 mm.

DISCUSSION

Shield

Due to the poor preservation of the shield, it is difficult to draw direct comparisons with other thylacocephalan species. Nevertheless, some morphological details require discussion.

Shape. A particular feature of the shield of *Concavicaris woodfordi* is the long shallow depression near the ventral margin (Figures 2C, 3D–F). This feature was previously described in the Devonian *Concavicaris bradleyi* (see Meek, 1872), and in the Carboniferous *Suttropcaris bottkei* Koch et al., 2003. More recently, it has been described in the Famennian *Concavicaris submarinus* (see Jobbins et al., 2020). The shield of *C. submarinus* shares many features with *C. woodfordi*: a straight anterior margin, convex dorsal midline and ventral margin, a rounded antero-ventral corner. Based on the few remains, the rostrum of *C. woodfordi* was probably similarly oriented (Figure 10). However, no posterior longitudinal depression was discovered on the shield of *C. woodfordi,* unlike *C. submarinus.*

Ornamentation. The presence of a serrate ridge on the dorsal area of the shield, also known in *Concavicaris elytroides* – the other thylacocephalan species described from the Woodford Shale – was reported by Cooper (1932). However, we did not see such a feature on the shield of this specimen.

Marginal fold. In many thylacocephalan species, a thickening of all free margins, or at least of the ventral margin, has been reported. A range of terminology has been used to describe such structure: flanges (Briggs and Rolfe, 1983), marginal carina (Arduini et al., 1980; Schram et al., 1999; Charbonnier et al., 2017), marginal belt (Charbonnier et al., 2019), marginal rim (Ji et al., 2017, 2021), or mar-

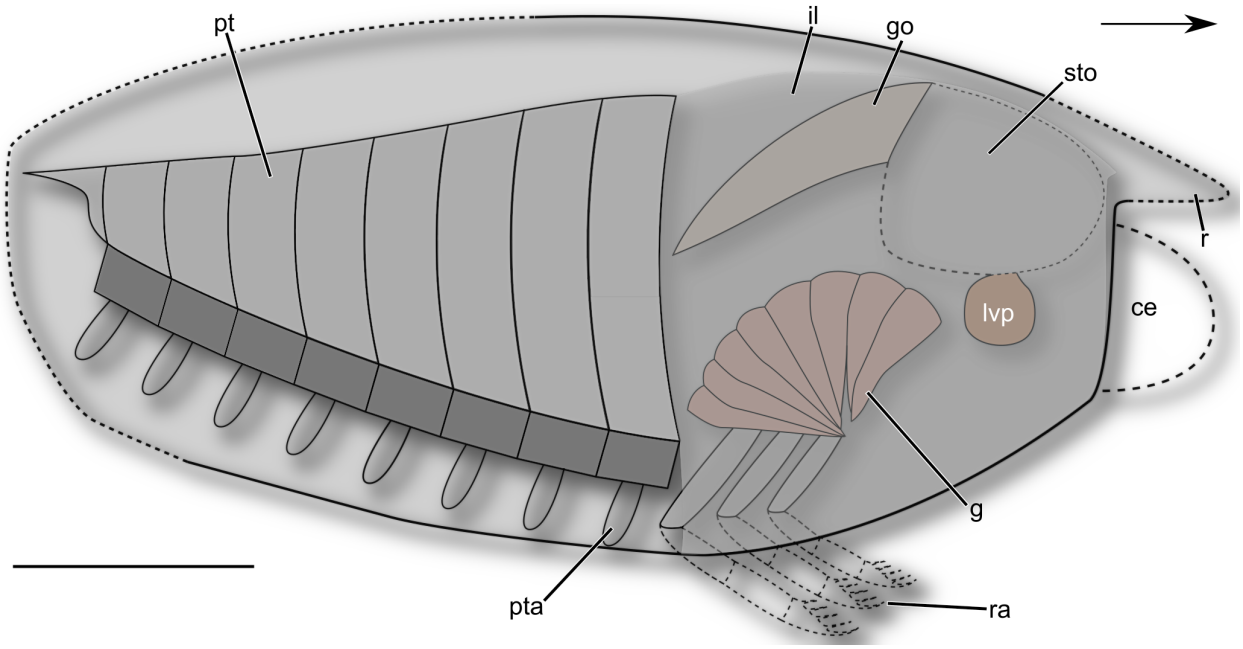

FIGURE 10. Hypothetical reconstruction of *Concavicaris woodfordi* (Cooper, 1932). Morphology of anterior and posterior sides of the shield, eyes and number of posterior trunk appendages are reconstructed based on *Concavicaris submarinus* (Jobbins et al., 2020). Abbreviations: ce, compound eyes; g, gills; go, gonads; il, inner layer: lvp, latero-ventral pouch; pt, posterior trunk; pta, posterior trunk appendages; r, rostrum; ra, raptorial appendages; s, shield; sto, stomach. Arrow indicates the anterior side of the specimen. Scales: 10 mm.

ginal fold (Laville et al., 2021a, 2021b) This structure, although often reported, has never been described in detail. In our CT-scans, we can clearly describe its morphology in *Concavicaris woodfordi:* it represents an inner folding of the shield (Figure 3). This marginal fold changes of morphology along the body: it appears thicker and higher in the anterior part of the shield, having a lunate shape in cross-section. In the posterior part, it has a triangular shape in cross-section and is less thick.

Inner folding of the shield is common in bivalved arthropods such as *Isoxys* (Fu et al., 2014), phosphatocopins (e.g., Zhang and Pratt, 2012), bradoriids (e.g., Betts et al., 2016), branchiopods (e.g., Fryer, 1996), podocopes (Yamada, 2007; Yamada and Keyser, 2010), and myodocopes (Yamada, 2019). In recent ostracods, the marginal infold brings more strength to the free margin shield, which might provide more stability to the organism (Benson, 1981). The marginal infold might also act as a barrier, protecting the soft-parts when the shield is closed (Betts et al., 2016). The marginal fold of thylacocephalans might have had a similar function, although we note that there is no clear evidence that thylacocephalans could have entirely closed their shield.

In recent ostracods, the marginal infold is formed from the outer lamella of the shield (Yamada, 2007). In thylacocephalans, however, it is difficult to assess, whether the marginal fold originates from the outer or from the inner lamella.

Inner layer. This is the first time that an inner layer connected to the shield has been reported in Thylacocephala. This layer is divided into two parts (Figures 4, 5). The posterior part most probably represents posterior trunk segments based on its division into a dorsal (tergal) area, two lateral (pleural) areas and a ventral (sternal) area.

The anterior part has a different morphology: it mirrors the shape of the shield and is directly attached to the marginal fold. It could represent a part of an endoskeleton, as found in many euarthropods (e.g., Snodgrass, 1952; Manton, 1960; Pilgrim and Wiersma, 1963; Pilgrim, 1973; Secrétan-Rey, 2002; Bitsch and Bitsch, 2002; Shultz, 2007). The endoskeleton is a system of cuticular ingrowth and/or tendinous structures that serves as a site for muscle and appendages attachment (Bitsch and Bitsch, 2002). It is thought to be segmented, being formed of inter- and intra-segmental structures, similar to the axial skeleton of Decapoda (Figure 5G; Secrétan-Rey, 2002). The inner layer of *Concavicaris woodfordi* does not

appear segmented and seems less complex in terms of morphology than the endoskeleton of other euarthropods. These differences make unlikely that this layer is part of an endoskeleton.

Instead, we suggest it likely represents a non-mineralized inner lamella, as found in the dorsal shield of bradoriids (Betts et al., 2016), branchiopods (Walossek, 1993; Fryer, 1996), myodocopes (Vannier and Abe, 1992; Abe and Vannier, 1995), podocopes, phosphatocopins (Müller et al., 2009; Zhang and Pratt, 2012), and tuzoiids (Ma et al., 2022). In those taxa, the dorsal integument is folded, forming a dorsal shield made of two layers: a calcified outer lamella and a generally non-mineralized, inner lamella (Figure 5H, I). One detail might prevent us from interpreting the inner layer of thylacocephalans as a non-mineralized inner lamella. As mentioned in the taphonomy section, this structure is formed of two dense layers, surrounding sediments. This looks inconsistent with the non-mineralized nature of the inner lamella of other euarthropods. However, the inner layer of phosphatocopines is often preserved as a mold, with two dense, phosphatic coating layers surrounding void (Müller, 1979; Olempska and Wacey, 2016). This appears similar to what we observed in *Concavicaris woodfordi:* the two dense layers are coating layers that surround sediments. The sediments most probably replaced the original inner layer, which was dissolved. Thus, we interpret the structure found in *C. woodfordi* as a non-mineralized inner layer.

This inner layer often plays a role in gaseous exchanges such as in Myodocopa. In this taxon, the inner layer is associated with a complex system of hemolymphatic sinuses, which are important for gaseous circulation through the body (Abe and Vannier, 1995; Williams et al., 2011). Vannier et al. (2016) suggested that *Dollocaris ingens* had a complex hemolymph circulatory system formed of a heart, of gills and of vessels associated with gaseous exchange and diffusion through an integumental network of the shield. If this network exists, it is probably associated with the inner layer as in Myodocopa. In *Concavicaris woodfordi*, the inner layer appears related to the various organs preserved, especially the gills, which can be important for gaseous exchange.

Digestive System

The association of a semi-circular structure with two latero-ventral rounded structures recalls part of the digestive system of *Dollocaris ingens* described by Vannier et al. (2016: figure 1). *Dollocaris ingens* possesses a cylindrical cardiac stomach connected to two latero-ventral pouches, a pyloric stomach associated with a bilobate hepatopancreas and an oval hindgut.

The latero-ventral pouches of *Concavicaris woodfordi* resemble those of *D. ingens*. Moreover, they are connected to the semi-circular structure which most probably corresponds to remain of the stomach. No other features of the digestive system have been reported in *C. woodfordi.*

Reproductive System

Similar plate-like structures to those of *Concavicaris woodfordi* (Figure 7) have been reported by Jobbins et al. (2020: figure 4e, f) in the dorsal part of the shield of *Concavicaris submarinus*, and interpreted as gonads or hepatopancreas. In *C. woodfordi*, even though they appear connected dorsally to the stomach, it is unlikely that those structures are the hepatopancreas. Vannier et al. (2016) described in *Dollocaris ingens* the hepatopancreas, which is located ventrally, surrounding the pyloric stomach. This is not the case of the plate-like structures of the Devonian representatives. Moreover, those structures do not have the typical tubular structure of the pancrustacean hepatopancreas.

We recently re-studied specimens of *D. ingens* using X-ray microtomography and noticed the presence of both organs in the same specimen (work in progress): the hepatopancreas, located ventrally, and the plate-like structures, located dorsally. This confirms that those later are not the hepatopancreas and might therefore be gonads as suggested by Jobbins et al. (2020).

Circulatory and Respiratory Systems

Gills. We herein reported eight pairs of lamellar structures (Figure 7E–G). Those elongate lamellar structures clearly resemble the set of gills of thylacocephalans. They have similar shape and position as the gills reported for *Concavicaris submarinus* (see Jobbins et al., 2020). Thus, we interpret those structure as gills. Jobbins et al. (2020: figure 4A, B) only reported three pairs of gills. Looking at the CT-scans and 3D rendering of *C. submarinus*, it is probable that some gills have been confused with gastric muscles in this species. Indeed, some of the putative lateral gastric muscles are in the same position as some of the most anterior gills of *C. woodfordi*.

The gills reported in Paleozoic thylacocephalans (e.g., Rolfe, 1985; Jobbins et al., 2020) are often small relative to the shield, when com-

pared to Mesozoic representatives (e.g., Arduini et al., 1980; Vannier et al., 2016). This difference in gills size might be the result of different lifestyles. If Mesozoic thylacocephalans had a more active lifestyle, they would probably have higher oxygen requirements. A way to fulfill those requirements would be to increase the exchange surface, and therefore the gill surface area. Such mechanisms have been suggested for extant pancrustaceans (e.g., Johnson and Rees, 1988; Glazier and Paul, 2017). For thylacocephalans, more comparative and morpho-functional studies will be required to conclude whether this difference is linked to a change in the mode of life.

Circulatory system. In the left part of the shield, a longitudinal cylindrical structure appears closely associated with the gills (Figure 7E–G). Based on its relationship with the gills, it could represent a structure for the attachment and support of the gills. However, the gills appear clearly attached to the inner layer, making it unlikely for this structure to serve as an attachment site. Instead, it might be a part of the circulatory system. In pancrustaceans (Wirkner and Richter, 2013), gills are usually associated with hemolymphatic sinuses that channel the hemolymph out of gills into the pericardial sinus and then into the heart. This cylindrical structure, which has a vessel-like morphology, is most probably part of these sinus networks.

Muscles

Gastric muscles. Based on their fibrous and elongate nature (Figure 8A–C), the anterior fibrous structures are most likely muscles. Their association with the putative stomach and the latero-ventral pouches implies that they are probably related to the digestive system. Moreover, they resemble in shape and location the central gastric muscles described in *Concavicaris submarinus* (see Jobbins et al., 2020). Gastric muscles are common in pancrustaceans (e.g., Kunze, 1981; Schmitz and Scherrey 1983; McGaw and Curtis 2013; Keiler et al., 2016). In such organisms, they surround the stomach and are closely related to it. We thus interpret the anterior fibrous structures as gastric muscles.

Adductor muscles. The fibrous nature of the central fibrous structures suggest that they are likely muscles (Figure 8D, E). Those muscles are connected to the shield and thus, might represent adductor muscles. Indeed, the presence of adductor muscles have often been suggested in thylacocephalans. In many species, large rounded spots located in the anterior or central part of the shield have been described as putative muscle scars. (Secrétan and Riou, 1983; Pinna et al., 1985; Secrétan, 1985; Charbonnier et al., 2017, 2019; Laville et al., 2021a). Moreover, those muscle scars can be associated with muscles, as for *Ostenocaris cypriformis* Arduini, Pinna and Teruzzi, 1980 from the Early Jurassic of Italy (Arduini et al., 1980; Pinna et al., 1985). The adductor muscles reported by Pinna et al. (1985) clearly resemble in terms of shape and position the central fibrous structures of *C. woodfordi*. Thus, we interpret those structure as adductor muscles.

Appendages

Raptorial appendages. Three long rectangular structures are visible in the central part of the shield, posterior to the set of gills (Figure 9A, B). The most anterior structure appears to be divided into at least two podomeres. This indicates that these structures are likely segmented. Based on their position, their orientation and their segmented nature, they might represent the proximal part of the raptorial appendages. Preservation of raptorial appendages is quite rare among Devonian thylacocephalans, for which only traces have been recorded (Broda et al., 2020).

The position of the raptorial appendages, which are related to the inner layer of the shield, and not to the posterior trunk, indicates that they are part of a more anterior tagma than the one of the posterior trunk appendages.

Posterior trunk appendages. The paddle-like structures associated with the posterior trunk are similar to the posterior trunk appendages described for *Concavicaris submarinus* and are thus interpreted as such (Figure 9C–E). Paddle-like appendages are quite common in Paleozoic taxa (Haug et al., 2014; Broda et al., 2020). It is, therefore, not surprising to recover a similar morphology in *Concavicaris woodfordi.*

Tagmatization

There are several major questions surrounding the character and mode of tagmatization in Thylacocephala (e.g., Polz, 1993). Multiple hypotheses have been made concerning this topic (see Laville et al., 2021a for a review); the main differences between them center on four major aspects: 1) the origin of the shield, 2) the number and nature of cephalic and posterior trunk appendages, 3) the nature of raptorial appendages, and 4) the insertion of gills.

Our work provides some insight to resolve the issue of thylacocephalan tagmatization (Figure 10).

First, we can confirm that thylacocephalans are at least divided into two regions. The first one corresponds to the shield with the raptorial appendages shown to belong to this region. Those appendages have been proposed as belonging to the cephalon (e.g., Vannier et al., 2016) or the anterior trunk (e.g., Rolfe, 1985). In *C. woodfordi*, they seem to be inserted into the posterior part of the shield, which might indicate an anterior trunk affinity. However, as the exact origin and segmentation of the shield is unknown, further discussion is not possible.

Another important structure – the gills – are shown to be attached to the lateral sides of shield, indicating that they are pleurobranchs. This confirms a hypothesis proposed by Schram and Koenemann (2022), but also confirms that they are not related to the posterior trunk, which corresponds to the second region of thylacocephalans.

CONCLUSION

Our study of *Concavicaris woodfordi* based on µCT imagery provides new insights into the anatomy of thylacocephalans. Our CT scans reveal new anatomical details, including the structure of the shield, the circulatory, digestive and reproductive systems, and the appendages. A marginal fold of the shield as well as an inner layer are described for the first time in a thylacocephalan. These data illustrate that *Concavicaris woodfordi* shares similarities with *Concavicaris submarinus*, another Famennian species, including the morphology of the shield and the internal anatomy. *Concavicaris woodfordi* also displays an organisation similar to Mesozoic taxa, such as *Dollocaris ingens*, although we note that the gills are smaller in *C. woodfordi*, potentially indicating variation in the mode of life of thylacocephalans. Our study does not entirely resolve the puzzle of thylacocephalan anatomy but does provide new important information that will be crucial to reconstructing the evolution and the affinities of this group.

ACKNOWLEDGEMENT

We would like to thank N. Poulet-Crovisier and F. Goussard (MNHN, Paris) for their help during the processing and the segmentation of the scans. We also thank M. Florence (USNM, Washington, DC) for his help with tracking down the specimen at the Smithsonian institution. We finally acknowledge the editor, L. Laibl, and the two anonymous reviewers for their comments that greatly improved the manuscript.

REFERENCES

Abe, K. and Vannier, J. 1995. Functional morphology and significance of the circulatory system of Ostracoda, exemplified by *Vargula hilgendorfii* (Myodocopida). Marine Biology, 124:51-58. https://doi.org/10.1007/BF00349146

Arduini, P., Pinna, G., and Teruzzi, G. 1980. A new and unusual Lower Jurassic cirriped from Osteno in Lombardy: *Ostenia cypriformis* n. g., n. sp.: preliminary note. Atti della Società italiana di scienze naturali e del Museo civico di storia naturale di Milano, 121:360-370.

Barrande, J. 1872. Systême Silurien du centre de la Bohême: Ière. Partie: Recherches Paléontologiques. Supplément au Vol. I. Trilobites, Crustacés divers et Poissons. Chez l'auteur, Prague.

Benson, R.H. 1981. Form, function, and architecture of ostracode shells. Annual Review of Earth and Planetary Sciences, 9:59-80. https://doi.org/10.1146/annurev.ea.09.050181.000423

Betts, M.J., Brock, G.A., and Paterson, J.R. 2016. Butterflies of the Cambrian benthos? Shield position in bradoriid arthropods. Lethaia, 49:478-491. https://doi.org/10.1111/let.12160

Bitsch, C. and Bitsch, J. 2002. The endoskeletal structures in arthropods: cytology, morphology and evolution. Arthropod Structure & Development, 30:159-177. https://doi.org/10.1016/S1467-8039(01)00032-9

Briggs, D.E.G. and Rolfe, W.D.I. 1983. New Concavicarida (new order:? Crustacea) from the Upper Devonian of Gogo, Western Australia, and the palaeoecology and affinities of the group. Special Papers in Palaeontology, 30:249-276.

Broda, K., Rak, Š., and Hegna, T.A. 2020. Do the clothes make the thylacocephalan? A detailed study of Concavicarididae and Protozoeidae (?Crustacea, Thylacocephala) carapace microornamentation. Journal of Systematic Palaeontology, 18: 911-930. https://doi.org/10.1080/14772019.2019.1695683

Broda, K. and Zatoń, M. 2017. A set of possible sensory system preserved in cuticle of Late Devonian thylacocephalan arthropods from Poland. Historical Biology, 29:1045-1055. https://doi.org/10.1080/08912963.2017.1284834

Charbonnier, S., Teruzzi, G., Audo, D., Lasseron, M., Haug, C., and Haug, J.T. 2017. New thylacocephalans from the Cretaceous Lagerstätten of Lebanon. Bulletin de la Société géologique de France, 188:19. https://doi.org/10.1051/bsgf/2017176

Charbonnier, S., Brayard, A., and The Paris Biota team. 2019. New thylacocephalans from the Early Triassic Paris Biota (Bear Lake County, Idaho, USA). Geobios, 54:37-43. https://doi.org/10.1016/j.geobios.2019.04.005

Chlupáč, I. 1963. Phyllocarid crustaceans from the Silurian and Devonian of Czechoslovakia. Palaeontology, 6:97-118.

Cignoni, P., Callieri, M., Corsini, M., Dellepiane, M., Ganovelli, F., and Ranzuglia, G. 2008. MeshLab: an Open-Source Mesh Processing Tool. Eurographics Italian Chapter Conference, p. 129-136. https://doi.org/10.2312/LocalChapterEvents/ItalChap/ItalianChapConf2008/129-136

Cooper, C.L. 1932. A crustacean fauna from the Woodford Formation of Oklahoma. Journal of Paleontology 6:346-352.

Feldmann, R.M. and Schweitzer, C.E. 2010. The oldest shrimp (Devonian: Famennian) and remarkable preservation of soft tissue. Journal of Crustacean Biology, 30:629-635. https://doi.org/10.1651/09-3268.1

Fryer, G. 1996. The carapace of the branchiopod Crustacea. Philosophical Transactions of the Royal Society of London. Series B: Biological Sciences, 351:1703-1712. https://doi.org/10.1098/rstb.1996.0152

Fu, D., Zhang, X., Budd, G.E., Liu, W., and Pan, X. 2014. Ontogeny and dimorphism of *Isoxys auritus* (Arthropoda) from the Early Cambrian Chengjiang biota, South China. Gondwana Research, 25:975-982. https://doi.org/10.1016/j.gr.2013.06.007

Glaessner, M.F. 1969. Decapoda, p. R400-R533. In Moore, R.C. (ed.), Treatise on Invertebrate Paleontology, Part R, Arthropoda 4. Geological Society of America and University of Kansas Press, Boulder, Colorado, and Lawrence, Kansas.

Glazier, D.S. and Paul, D.A. 2017. Ecology of ontogenetic body-mass scaling of gill surface area in a freshwater crustacean. Journal of Experimental Biology, 220:2120-2127. https://doi.org/10.1242/jeb.155242

Haug, C., Briggs, D.E.G., Mikulic, D.G., Kluessendorf, J., and Haug, J.T. 2014. The implications of a Silurian and other thylacocephalan crustaceans for the functional morphology and systematic affinities of the group. BMC Evolutionary Biology, 14: 159. https://doi.org/10.1186/s12862-014-0159-2

Heidtke, U.H.J. and Krätschmer, K. 2001. Ein Fragment von *Ainiktozoon* aus dem Oberdevon der Bergisch Gladbach-Paffrath Mulde (Rheinisches Schiefergebirge, Deutschland). Neues Jahrbuch für Geologie und Paläontologie – Monatshefte, 2001:233-236. https://doi.org/10.1127/njgpm/2001/2001/233

Hilgendorf, F. 1885. Ueber cretacische Squilliden-Larven vom Libanon. Sitzungs-Berichte der Gesellschaft naturforschender Freunde zu Berlin, 1885:184-185.

Ji, C., Tintori, A., Jiang, D., and Motani, R. 2017. New species of Thylacocephala (Arthropoda) from the Spathian (Lower Triassic) of Chaohu, Anhui Province of China. PalZ, 91:171-184. https://doi.org/10.1007/s12542-017-0347-7

Ji, C., Tintori, A., Jiang, D., Motani, R., and Confortini, F. 2021. New Thylacocephala (Crustacea) assemblage from the Spathian (Lower Triassic) of Majiashan (Chaohu, Anhui Province, South China). Journal of Paleontology, 95:305-319. https://doi.org/10.1017/jpa.2020.92

Jobbins, M., Haug, C., and Klug, C. 2020. First African thylacocephalans from the Famennian of Morocco and their role in Late Devonian food webs. Scientific Reports, 10:5129. https://doi.org/10.1038/s41598-020-61770-0

Johnson, L. and Rees, C.J.C. 1988. Oxygen consumption and gill surface area in relation to habitat and lifestyle of four crab species. Comparative Biochemistry and Physiology Part A: Physiology, 89:243-246. https://doi.org/10.1016/0300-9629(88)91086-9

Keiler, J., Richter, S., and Wirkner, C.S. 2016. Revealing their innermost secrets: an evolutionary perspective on the disparity of the organ systems in anomuran crabs (Crustacea: Decapoda: Anomura). Contributions to Zoology, 85:361-386. https://doi.org/10.1163/18759866-08504001

Kirkland, D.W., Denison, R.E., Summers, D.M., Gormly, J.R., Johnson, K.S., and Cardott, B.J. 1992. Geology and organic geochemistry of the Woodford Shale in the Criner Hills and western Arbuckle Mountains, Oklahoma. Oklahoma Geological Survey Circular, 93:38-69.

Koch, L., Gröning, E., and Brauckmann, C. 2003. Suttropcarididae n. fam. (Phyllocarida, Crustacea) aus dem Ober-Devon des Sauerlandes (Rheinisches Schiefergebirge, Deutschland). Neues Jahrbuch für Geologie und Paläontologie – Monatshefte, 2003:415-427. https://doi.org/10.1127/njgpm/2003/2003/415

Kunze, J. 1981. The functional morphology of stomatopod Crustacea. Philosophical Transactions of the Royal Society of London. B, Biological Sciences, 292:255-328. https://doi.org/10.1098/rstb.1981.0032

Lange, S., Schram, F.R., Steeman, F.A., and Hof, C.H.J. 2001. New genus and species from the Cretaceous of Lebanon links the Thylacocephala to the Crustacea. Palaeontology, 44:905-912. https://doi.org/10.1111/1475-4983.00207

Laville, T., Haug, C., Haug, J.T., Forel, M.-B., and Charbonnier, S. 2021a. Morphology and anatomy of the Late Jurassic *Mayrocaris bucculata* (Eucrustacea?, Thylacocephala) with comments on the tagmosis of Thylacocephala. Journal of Systematic Palaeontology, 19:289-320. https://doi.org/10.1080/14772019.2021.1910584

Laville, T., Smith, C.P.A., Forel, M.-B., Brayard, A., and Charbonnier, S. 2021b. Review of Early Triassic Thylacocephala. Rivista Italiana di Paleontologia e Stratigrafia, 127:73-101. https://doi.org/10.13130/2039-4942/15188

Ma, J.-X., Lin, W.-L., Liu C., Sun, A., Wu, Y., Wu, Y.-H., and Fu, D.-J. 2022. A new bivalved arthropod from Cambrian (Stage 3) Qingjiang biota expands the palaeogeographical distribution and increases the diversity of Tuzoiidae. Journal of the Geological Society 179: jgs2020-229. https://doi.org/10.1144/jgs2020-229

Manton, S.M. 1960. Concerning head development in the arthropods. Biological Reviews, 35:265-282. https://doi.org/10.1111/j.1469-185X.1960.tb01416.x

McGaw, I.J. and Curtis, D.L. 2013. A review of gastric processing in decapod crustaceans. Journal of Comparative Physiology B, 183:443-465. https://doi.org/10.1007/s00360-012-0730-3

Meek, F.B. 1872. Descriptions of new western Paleozoic fossils, mainly from the Cincinnati Group of the Lower Silurian Series of Ohio. Proceedings of the Academy of Natural Sciences of Philadelphia, 24:308-336.

Müller, K.J. 1979. Phosphatocopine ostracodes with preserved appendages from the Upper Cambrian of Sweden. Lethaia, 12:1-27. https://doi.org/10.1111/j.1502-3931.1979.tb01234.x

Müller, K., Waloszek, D., and Maas, A. 2009. Morphology, Ontogeny and Phylogeny of the Phosphatocopina (Crustacea) from the Upper Cambrian Orsten of Sweden. Fossil and Strata. John Wiley & Sons.

Olempska, E. and Wacey, D. 2015. Ambient inclusion trails in Paleozoic crustaceans (Phosphatocopina and Ostracoda). Palaeogeography, Palaeoclimatology, Palaeoecology, 441:949-958. https://doi.org/10.1016/j.palaeo.2015.10.052

Over, D.J. 1992. Conodonts and the Devonian-Carboniferous boundary in the upper Woodford Shale, Arbuckle Mountains, south-central Oklahoma. Journal of Paleontology, 66:293-311. https://doi.org/10.1017/S0022336000033801

Pilgrim, R.L.C. 1973. Axial skeleton and musculature in the thorax of the hermit crab, *Pagurus Bernhardus* [Anomura:Paguridae]. Journal of the Marine Biological Association of the United Kingdom, 53:363-396. https://doi.org/10.1017/S0025315400022335

Pilgrim, R.L.C. and Wiersma, C. A. G. 1963. Observations on the skeleton and somatic musculature of the abdomen and thorax of *Procambarus clarkii* (Girard), with notes on the thorax of *Panulirus interruptus* (Randall) and *Astacus*. Journal of Morphology, 113:453-487. https://doi.org/10.1002/jmor.1051130308

Pinna, G., Arduini, P., Pesarini, C., and Teruzzi, G. 1982. Thylacocephala: una nuova classe di crostacei fossili. Atti della Società italiana di Scienze naturali e del Museo civico di Storia naturale di Milano, 123:469-482.

Pinna, G., Arduini, P., Pesarini, C., and Teruzzi, G. 1985. Some controversial aspects of the morphology and anatomy of *Ostenocaris cypriformis* (Crustacea, Thylacocephala). Transactions of the Royal Society of Edinburgh: Earth Sciences, 76:373-379. https://doi.org/10.1017/S0263593300010580

Roberts, C.T., Mitterer, R.M., Johnson, K.S. and Cardott, B.J. 1992. Laminated black shale-bedded chert cyclicity in the Woodford Formation, southern Oklahoma. Source rocks in the southern Midcontinent, 1990 symposium: Norman, Oklahoma, Oklahoma Geological Society, Oklahoma Geological Survey Circular, 93:330-336.

Rolfe, W.D.I. 1985. Form and function in Thylacocephala, Conchyliocarida and Concavicarida (?Crustacea): a problem of interpretation. Transactions of the Royal Society of Edinburgh: Earth Sciences, 76:391-399. https://doi.org/10.1017/S0263593300010609

Rolfe, W.D.I. and Dzik, J. 2006. *Angustidontus*, a Late Devonian pelagic predatory crustacean. Earth and Environmental Science Transactions of The Royal Society of Edinburgh, 97:75-96. https://doi.org/10.1017/S0263593300001413

Romero, A.M. and Philp, R.P. 2012. Organic geochemistry of the Woodford Shale, southeastern Oklahoma: How variable can shales be? Organic Geochemistry of the Woodford Shale, Southeastern Oklahoma. AAPG Bulletin, 96:493-517. https://doi.org/10.1306/08101110194

Schmitz, E.H. and Scherrey, P.M. 1983. Digestive anatomy of *Halella azteca* (Crustacea, Amphipoda). Journal of Morphology, 175:91-100. https://doi.org/10.1002/jmor.1051750109

Schneider, C.A., Rasband, W.S., and Eliceiri, K.W. 2012. NIH Image to ImageJ: 25 years of image analysis. Nature Methods, 9:671-675. https://doi.org/10.1038/nmeth.2089

Schram, F.R. 2014. Family level classification within Thylacocephala, with comments on their evolution and possible relationships. Crustaceana, 87:340-363. https://doi.org/10.1163/15685403-00003289

Schram, F.R., Hof, C.H.J., and Steeman, F.A. 1999. Thylacocephala (Arthropoda: Crustacea?) from the Cretaceous of Lebanon and implications for thylacocephalan systematics. Palaeontology, 42:769-797. https://doi.org/10.1111/1475-4983.00097

Schram, F.R. and Koenemann, S. 2022. Infraclass Thylacocephala, p. 603-624. Evolution and Phylogeny of Pancrustacea: A Story of Scientific Method. Oxford University Press, New York.

Secretan, S. 1985. Conchyliocarida, a class of fossil crustaceans: relationships to Malacostraca and postulated behaviour. Transactions of the Royal Society of Edinburgh: Earth Sciences, 76:381-389. https://doi.org/10.1017/S0263593300010592

Secretan, S. and Riou, B. 1983. Un groupe énigmatique de Crustacés: ses représentants du Callovien de la Voulte-sur-Rhône (France). Annales de Paléontologie, 69:59-97.

Secretan-Rey, S. 2002. Monographie du squelette axial de *Nephrops norvegicus* (Linné, 1758). Zoosystema, 24:81-176.

Shultz, J.W. 2007. Morphology of the prosomal endoskeleton of Scorpiones (Arachnida) and a new hypothesis for the evolution of cuticular cephalic endoskeletons in arthropods. Arthropod Structure & Development, 36:77-102. https://doi.org/10.1016/j.asd.2006.08.001

Snodgrass, R.E. 1952. Textbook of Arthropod Anatomy. Cornell University Press, Ithaca, New York.

Stigall, A.L. and Hendricks, J.R. 2007. First report of a concavicarid interior (Crustacea: Thylacocephala) from the Devonian of North America. Northeastern Geology and Environmental Sciences, 29:102-106.

Van Straelen, V. 1923. Les mysidacés du Callovien de la Voulte-sur-Rhône. Bulletin de la Société Géologique de France, 23:431-439.

Vannier, J. and Abe, K. 1992. Recent and early Paleozoic myocodope ostracodes: functional morphology, phylogeny, distributions and lifestyles. Palaeontology, 35:485-517.

Vannier, J., Schoenemann, B., Gillot, T., Charbonnier, S., and Clarkson, E. 2016. Exceptional preservation of eye structure in arthropod visual predators from the Middle Jurassic. Nature Communications, 7: 10320. https://doi.org/10.1038/ncomms10320

Walossek, D. 1993. The Upper Cambrian *Rehbachiella* and the phylogeny of Branchiopoda and Crustacea. Lethaia, 26:318-318. https://doi.org/10.1111/j.1502-3931.1993.tb01537.x

Williams, M., Vannier, J., Corbari, L., and Massabuau, J.-C. 2011. Oxygen as a driver of early arthropod micro-benthos evolution. PLoS ONE, 6:e28183. https://doi.org/10.1371/journal.pone.0028183

Wirkner, C.S. and Richter, S. 2013. Circulatory system and respiration, p. 376-412. In Watling, L. and Thiel, L. (eds.), Functional Morphology and Diversity. Natural History of Crustacea. Oxford University Press, New York, NY. https://doi.org/10.1093/acprof:osobl/9780195398038.003.0014

Yamada, S. 2007. Ultrastructure of the carapace margin in the Ostracoda (Arthropoda: Crustacea), p. 201-211. In Matzke-Karasz, R., Martens, K., and Schudack, M. (eds.), Ostracodology — Linking Bio- and Geosciences. Developments in Hydrobiology. Springer

Netherlands, Dordrecht. https://doi.org/10.1007/978-1-4020-6418-0_15
Yamada, S. 2019. Ultrastructure and cuticle formation of the carapace in the myodocopan ostracod exemplified by *Euphilomedes japonica* (Crustacea: Ostracoda). Journal of Morphology, 280:809-26. https://doi.org/10.1002/jmor.20985
Yamada, S. and Keyser, D. 2010. Calcification of the marginal infold in podocopid ostracods. Hydrobiologia, 638:213-222. https://doi.org/10.1007/s10750-009-0042-0
Zatoń, M., Filipiak, P., Rakociński, M., and Krawczyński, W. 2014. Kowala Lagerstätte: Late Devonian arthropods and non-biomineralized algae from Poland. Lethaia, 47:352-364. https://doi.org/10.1111/let.12062
Zhang, X. and Pratt, B.R. 2012. The first stalk-eyed phosphatocopine Crustacean from the Lower Cambrian of China. Current Biology, 22:2149-2154. https://doi.org/10.1016/j.cub.2012.09.027
Zrzavý, J. and Štys, P. 1997. The basic body plan of arthropods: insights from evolutionary morphology and developmental biology. Journal of Evolutionary Biology, 10:353-367. https://doi.org/10.1046/j.1420-9101.1997.10030353.x

APPENDICES

APPENDIX 1. Tomograms, Mimics (segmentation) and STL files (3D rendering). Please download 1218_appendices.zip at https://palaeo-electronica.org/content/2022/3735-new-look-at-concavicaris-woodfordi.

APPENDIX 2. 3D rendering of *Concavicaris woodfordi* based on the segmentation. For animated version, please download 1218_appendices.zip at https://palaeo-electronica.org/content/2022/3735-new-look-at-concavicaris-woodfordi.

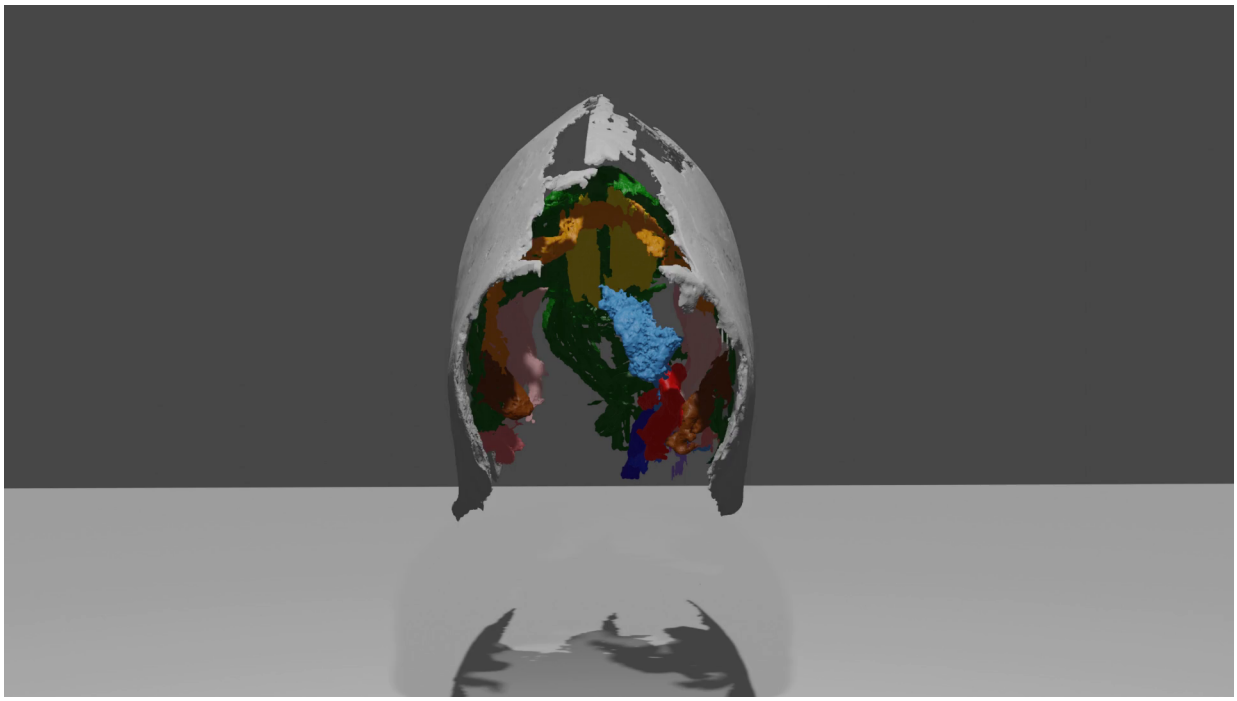

The data for the Appendices can also be downloaded at the following link: https://doi.org/10.5281/zenodo.5913066